The Energetic Benefit of Robotic Gait Selection - A Case Study on the Robot RAM*one* -

Nils Smit-Anseeuw, Rodney Gleason, Ram Vasudevan, and C. David Remy .

***Abstract*—Should a legged robot use different gaits at different desired speeds? If so, what constitutes these gaits? This work examines these questions through a case study on the planar bipedal robot RAM*one*. Using a realistic model of the robot, this paper presents the outcome of a series of trajectory optimizations which minimize the electrical cost of transport and find the associated optimal motion strategies. These optimizations show that at low speeds it is most economical to perform a ballistic walking gait with an instantaneous transfer of support. At higher speeds, spring-mass running with an extended air-phase becomes the optimal gait. Additionally, it is illustrated that the optimal running gait is conducted with the knee joints pointing away from rather than towards the direction of travel. The transition between ballistic walking and spring-mass running happens at a speed of 1.04 m/s, and switching can reduce energy expenditure by up to 259 %.**

***Index Terms*—Humanoid and Bipedal Locomotion; Optimization and Optimal Control; Biologically-Inspired Robots**

I. Introduction

BEING able to move in an energetically economical fashion over a wide range of velocities is a desirable property for legged robotic systems. Imagine, for example, an autonomous search and rescue robot. This robot would ideally operate in at least two distinct locomotor modes: a fast traveling mode to quickly get to the disaster scene, and a slow exploration mode that is employed at the scene while searching for survivors. Efficiency is key in either mode to maximize the operation time and range of the robot.

Similarly, biological systems need to move efficiently over a wide range of speeds. They achieve this energetic economy by using different gaits, such as walking, running, or galloping. By switching between gaits, animals and humans travel across a large range of speeds in an energetically economical manner [1], [2]. This paper asks if the ability to change gaits can lead to a similarly improved energetic economy in a bipedal robot and investigates the nature of these gaits.

One way to gain insight into the mechanisms that govern locomotor economy is to study the characteristic properties of biological gaits. The simplest such property is the contact pattern; that is, the sequence in which feet strike and leave the ground [3]. Another property consists of the phase relationship of kinetic and potential energy during locomotion. This phase relationship has been shown to be distinctly different at low and high speeds across a large range of species [4]. Another such property which characterizes gait is the shape of the contact force profiles, which has been used to classify gaits into walking or running [5]. In fact, as locomotion speed varies in animals, the type of locomotion (as classified by each of these gait characteristics) also changes [1], [4], [5].

If economical locomotion in robotic systems similarly varied as a function of speed, controller design would be profoundly impacted. Since different gaits constitute distinct motions which do not continuously transition from one to another, economical robot locomotion would require controllers that discretely switched from one gait to another. As a result, the question of the existence and the energetic benefits of distinct gaits is fundamentally important to the robotics community.

The extension of gait from biology to robotics is nontrivial, since biological and artificial systems are fundamentally dissimilar. To establish a meaningful connection between nature and robotics, a number of simple models have been proposed that provide a useful interface between biology and machine. They distill fundamental principles from locomotion in nature to provide templates for design and control of robots. Such models include a point mass on massless legs [8], passive

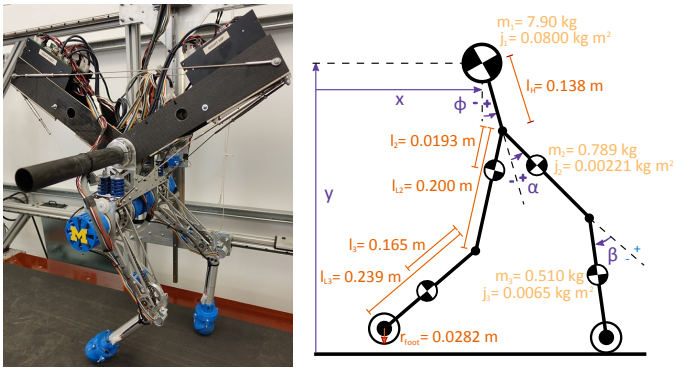

Fig. 1. This paper uses optimal control to find energetically efficient gaits for the robot RAM*one*. This robot was built to explore the exploitation of natural dynamics in legged locomotion. It is based on the Scarl*ETH* leg design [6], driven by series elastic actuators, and mounted on a planarizer which restricts its motion to the sagittal plane [7]. The robot is represented as a detailed five link planar model. The model uses a floating base description with rigid rolling contacts, it encodes the actuator dynamics with non-linear springs, and accounts for dry friction and viscous damping in the joints. All parameters are given in a supplementary MATLAB script `Parameters.m`.

Manuscript received: September, 10, 2016; Revised December, 4, 2016; Accepted January, 20, 2017.

This paper was recommended for publication by Editor Nikos Tsagarakis upon evaluation of the Associate Editor and Reviewers' comments. We would like to thank Kevin Green for his help in characterizing RAM*one* and Petr Zaytsev for his contributions to the manuscript. This material is based upon work supported by the National Science Foundation under Grant No. 1453346 and 1562612. Any opinion, findings, and conclusions or recommendations expressed in this material are those of the authors and do not necessarily reflect the views of the National Science Foundation.

The authors are with the Department of Mechanical Engineering, University of Michigan, Ann Arbor, MI {nilssmit,gleasonr,ramv,cdremy}@umich.edu

Digital Object Identifier (DOI): see top of this page.

dynamic walkers [9], the spring loaded inverted pendulum [10], and elastic walking models [11], [12].

To strengthen the link between these simple models and actual robotic systems, this paper investigates a set of optimal motions for a specific robotic system (Fig. I). RAM*one* is a bipedal robot, designed specifically to investigate energy efficiency and the role of gaits in robotic hardware. The robot is driven by high compliance series elastic actuators that can store large amounts of elastic energy and thus enable locomotion that exploits natural dynamics [13]. This paper investigates properties of the energetically optimal motion at different speeds and determines whether using distinct gaits is useful for a robotic system and whether certain gait characteristics from biology or conceptual models are applicable to RAM*one*. Though this work focuses on illustrating the benefits of using distinct gaits at varying speeds on this particular robot, the presented approach clears the path for future hardware experiments since the developed model is realistic. In fact, robots with similar design and actuation will show similar characteristics and the proposed methods can be extended to other legged robotic systems.

The investigation in this paper can be seen as an extension of previous work in optimal gait for conceptual models [14], [13], [15], [16] and builds upon optimization methodologies put forward in [17], [18], [19]. This paper presents optimization across a variety of speeds for two distinct contact sequences and two different knee orientations. In addition to the added detail and realism that comes from modeling an actual robot rather than a contrived conceptual model, some of the important differences between this and previous work stem from the inclusion of articulating knees with nonlinear springs, and the presence of a large reflected inertia in the motors.

The remainder of this paper introduces the model, the cost function, and the employed optimal control approach (Section II), and classifies and discusses the obtained motions (Sections III and IV). In particular, we show that for RAM*one* the most efficient motions are ballistic walking at slow speeds and spring-mass running at high speeds. Furthermore, we show that it is clearly beneficial for RAM*one* to run with its knees pointing backwards. These results are put in context with findings from nature and with prior work on simple models. To the best of our knowledge, this is the most realistic model of a robotic system for which the benefits of changing gait have been demonstrated.

II. Constructing Optimal Motions

This paper exploits trajectory optimization to discover energetically economic motions for the robot RAM*one* (Fig. I). RAM*one* is a bipedal, five link, planar robot with circular feet and high-compliance series elastic actuators that are driven by brushless DC motors. It has the same legs as the Scarl*ETH* and Starl*ETH* robots [20], [21]. Since the robot has articulated knees, the presented approach considers motions for a pair of discrete morphologies: knees forward and knees backward with respect to the direction of motion. In addition, two different footfall patterns are evaluated. The first is a walking sequence with alternating single support and double support phases. The second is a running sequence in which phases of single support alternate with flight phases.

A. Model

The kinematic configuration, $\boldsymbol{q}$, of the model of RAM*one* was described by the main body position x and y, the main body orientation ϕ, the hip angles α_L and α_R, and the knee angles β_L and β_R. Since the robot is driven by series elastic actuators, four additional coordinates encoded the motor positions $u_{\alpha L}$, $u_{\alpha R}$, $u_{\beta L}$, and $u_{\beta R}$. A vector of motor torques $\boldsymbol{T}$ constitutes the input to this model. In the supplementary documents[1], MATLAB code that defines the dynamics, cost, and constraints of this model is included. The following is an overview of the model, highlighting only important features.

1) Dynamics: To formulate the dynamics, a hybrid dynamic approach is employed[22] in which continuous dynamics are interrupted by discrete events, corresponding to feet gaining or losing contact with the ground. The mechanical dynamics $\ddot{\boldsymbol{q}} = \boldsymbol{f_c}(\boldsymbol{q}, \dot{\boldsymbol{q}}, \boldsymbol{\tau})$, were derived using implicitly constrained Newton-Euler equations. Here $\boldsymbol{\tau}$ represents the torques exerted on the joints by the actuators. In this approach, the generalized accelerations $\ddot{\boldsymbol{q}}$ and the contact forces $\boldsymbol{\lambda}$ are simultaneously solved for.

If a foot leaves the ground, the contact is removed from the set of active constraints which changes the structure of the mechanical dynamics but does not alter the state. When a foot comes into contact with the ground, a new constraint is established, and the foot is assumed to be instantaneously brought to a halt by a collision impulse $\boldsymbol{\Lambda}$. To this end, a discrete state transition $\dot{\boldsymbol{q}}^+ = \boldsymbol{f_d}(\boldsymbol{q}^-, \dot{\boldsymbol{q}}^-)$ is computed which expresses the generalized velocity after the event ($\dot{\boldsymbol{q}}^+$) based on the pre-impact state ($\boldsymbol{q}^-$ and $\dot{\boldsymbol{q}}^-$). When solving for $\dot{\boldsymbol{q}}^+$ and $\boldsymbol{\Lambda}$, one must carefully choose a post impact active constraint set that satisfies nonpenetration and nonnegative ground contact force conditions across the transition. In particular, this means that for the walking sequence (in which one foot is on the ground when the other collides), two outcomes are possible. Either the first foot remains on the ground, leading into an extended double-support phase, or the first foot immediately lifts off, creating an instantaneous double-support phase.

2) Series Elasticity: RAM*one* has two different types of series elastic springs, one type for the hip joints and the other for the knee joints [20]. The hip springs behave linearly with viscous damping and negligible dry friction. The resulting force model is:

$$\tau_\alpha = -k_\alpha \Delta\alpha - b_\alpha \Delta\dot{\alpha}, \tag{1}$$

where $\Delta\alpha = \alpha - u_\alpha$ is the difference between joint position and motor position, and τ_α is the torque on the hip joint.

To improve knee angle control while the foot is in the air, the robot's knees are designed with "endstops" in the series elastic knee springs [20]. The resulting knee joint is modeled as a position and velocity dependent spring damper system. When the knee joint is pushing against the endstop, we have a high stiffness and damping (k_β^1, b_β^1), otherwise they take

[1] https://bitbucket.org/ramlab/ral_2016

on smaller values (k^2_β, b^2_β). The dry friction (f_β) observed in experiment is added to the model to obtain the following nonlinear spring:

$$\begin{aligned}\tau_\beta = &- k^1_\beta \Delta\beta - (k^2_\beta - k^1_\beta)\min(0, \Delta\beta - \beta_{sm}) \\ &- b^2_\beta \Delta\dot{\beta} - (b^1_\beta - b^2_\beta)\Delta\dot{\beta}\mathbb{1}_{(\Delta\beta-\beta_{sm}>0)}\mathbb{1}_{(\Delta\dot{\beta}>0)} \\ &- f_\beta \operatorname{sign}(\Delta\dot{\beta}),\end{aligned} \tag{2}$$

where $\mathbb{1}_A$ is the indicator function over the set A, $\Delta\beta = \beta - u_\beta$ is the difference between the joint and motor position, and τ_β is the torque on the knee joint.

3) Motor Model: Each joint of RAM*one* is actuated by a brushless DC motor that is connected via a gearbox and chain drive to a series elastic spring. In the model considered in this paper, the motors are represented by their rotor inertia J_{rot}, the motor speed-torque gradient S_{mot}, and the net gear ratio of n_α and n_β for the hip and knee, respectively. Motor torques $\boldsymbol{T}$ and speeds $\dot{\boldsymbol{u}}$ are limited by the maximum rated continuous motor torque T^{max} and the maximum rated input speed of the gearboxes $\dot{u}^{max}$. In the series elastic actuators, the motor accelerations $\ddot{\boldsymbol{u}}$ are determined individually for each actuator:

$$n^2 J_{rot}\ddot{u} = (T - \tau). \tag{3}$$

All model parameters needed to compute the dynamics, cost, and constraints are provided in the supplementary MATLAB script `Parameters.m`. The parameters were identified and refined iteratively as the robot hardware was undergoing continuous testing and evaluation. The inertial properties were established from CAD models of RAM*one* and verified through measurement where possible. Other parameter values were determined using manufacturer specifications when available and were otherwise identified through direct or indirect measurement and fitting.

B. Optimization

Given this model, the following constrained optimization problem is solved to find the energetically economical periodic motions:

$$\begin{aligned}\min_{\boldsymbol{q},\dot{\boldsymbol{q}},\boldsymbol{u},\dot{\boldsymbol{u}},\boldsymbol{T},t_F} \quad & \text{CoT}(\boldsymbol{q},\dot{\boldsymbol{u}},\boldsymbol{T},t_F) && \text{(4a)}\\ \text{s.t. } & \text{Continuous Dynamics}(\boldsymbol{q},\dot{\boldsymbol{q}},\boldsymbol{u},\dot{\boldsymbol{u}},\boldsymbol{T}) && \text{(4b)}\\ & \text{Actuator Limits}(\boldsymbol{u},\dot{\boldsymbol{u}},\boldsymbol{T}) && \text{(4c)}\\ & \text{Joint Limits}(\boldsymbol{q}) && \text{(4d)}\\ & \text{Foot Nonpenetration}(\boldsymbol{q}) && \text{(4e)}\\ & \text{Positive Contact Force}(\boldsymbol{q},\dot{\boldsymbol{q}},\boldsymbol{u},\dot{\boldsymbol{u}}) && \text{(4f)}\\ & \text{Discrete Dynamics}\left(\boldsymbol{q}^-,\dot{\boldsymbol{q}}^-\right) && \text{(4g)}\\ & \text{Foot Touchdown}\left(\boldsymbol{q}^-,\dot{\boldsymbol{q}}^-\right) && \text{(4h)}\\ & \text{Positive Contact Impulse}\left(\boldsymbol{q}^-,\dot{\boldsymbol{q}}^-\right) && \text{(4i)}\\ & \text{Foot Liftoff}\left(\boldsymbol{q}^-,\dot{\boldsymbol{q}}^-\right) && \text{(4j)}\\ & \text{Periodicity}(\boldsymbol{q}(0),\dot{\boldsymbol{q}}(0),\boldsymbol{u}(0),\dot{\boldsymbol{u}}(0), \\ & \qquad \boldsymbol{q}(t_F),\dot{\boldsymbol{q}}(t_F),\boldsymbol{u}(t_F),\dot{\boldsymbol{u}}(t_F)) && \text{(4k)}\\ & \text{Fixed Speed}(\boldsymbol{q},t_F). && \text{(4l)}\end{aligned}$$

The motion obtained from this formulation represents an energetic optimum for uninterrupted periodic locomotion without external disturbances, model errors, and sensor noise. In particular, the results will not take into account the additional energetic cost associated with stabilizing feedback.

1) Cost Function: The cost function used in the optimization estimates the electrical work required to drive the motors. Its computation reflects the fact that the motors share an input voltage rail, such that electrical power generated from one motor can be directly consumed by the other motors. The total power is thus the sum of the mechanical motor power and the motor copper losses of all four motors i. Since the robot has no means to store excess electrical energy in batteries or capacitors, if all motors together create negative net power, this power is dissipated in the form of shunt losses. Negative values were thus excluded when power was integrated over a full stride with period t_F:

$$c = \int_0^{t_F} \max\left(\sum_{i=1}^{4} T_i\dot{u}_i + \frac{T_i^2}{n_i^2 S_{mot}}, 0\right) dt. \tag{5}$$

To compare energetic economy across different velocities, the resulting work was normalized to yield a dimensionless "cost-of-transport" (CoT) [23]:

$$CoT = \frac{c}{mg\Delta x}, \tag{6}$$

where Δx is the distance traveled in the stride and mg is the total weight of the robot.

2) Constraints: Mathematical constraints were used to ensure that the resulting motion was feasible on RAM*one*. These constraints fall into three categories: continuous constraints (Eqs.4b,4c,4d,4e,4f) which must be satisfied throughout the continuous phases of the trajectory, discrete constraints (Eqs.4g,4h,4i,4j) which must be satisfied during the event phases, and endpoint constraints (Eqs.4k,4l) which must be satisfied at the start and end of the trajectory. They encode the dynamics and physical limitations of the model, as well as the required periodicity and locomotion speed.

3) Optimizer: The constrained optimization problem in Eq. (4) was solved with the optimization package MUSCOD [24], [25], [26]. MUSCOD is a multistage multiple shooting optimizer that can perform simultaneous optimization of trajectories and control inputs for nonlinear systems with a predefined schedule of continuous modes. The trajectory and input are discretized as trajectory nodes with piecewise constant control inputs. Between nodes, the dynamics are integrated forwards with variable step integration, providing feasible trajectories even with coarse discretization. Additionally, MUSCOD allows for nonlinear state and input constraints throughout the trajectory.

Optimizations were performed for two distinct footfall sequences: a walking sequence and a running sequence. For the walking sequence, two possible collision outcomes had to be accounted for. In one outcome, the stance foot remains on the ground when the swing foot impacts which results in a double stance phase of finite duration. In the other, the stance foot immediately lifts off, resulting in a zero duration double stance phase. Also, rather than implementing two models for the different knee directions, optimizations were conducted for positive and negative velocities.

Since this optimization is not necessarily convex, initialization is an important consideration when searching for global optima. The search for walking sequence trajectories was initialized with a feasible walking gait generated with a hand built controller. This gait contained a significant double support phase. The search for running sequence trajectories was initialized with a stationary trajectory. Once an optimal trajectory was found at a single velocity, this trajectory was used to initialize optimizations at higher and lower velocities. This process was repeated recursively. Optimizations were undertaken for the running and walking sequences and with the knees pointing forwards and backwards over a range of locomotion velocities with a velocity resolution of 0.02 m/s.

III. Optimal Motions and Gaits

Results of the optimizations are presented in Fig. 2. For a range of speeds, each curve shows the cost of transport (CoT) of the optimal motion for a given sequence and knee orientation. Note that attempts to enforce a non-zero duration double-stance in walking inevitably led to a higher CoT (Fig. 2). Hence, this paper will focus solely on the walking sequence solutions with an instantaneous transfer of support.

At low speeds, motions with a walking sequence are found to be optimal, while at high speeds a running sequence consumes less energy. The transition happens at 1.04 m/s. Below this speed, three of the four motions exhibit a ballistic walking gait (Sec. III-A), while above this speed the two running sequence motions exhibit a spring mass running gait (Sec. III-B). The differences in cost are small below the transition speed, but clearly deviate for higher speeds. At these higher speeds, a significant benefit of having the knees pointing backwards rather than forwards is observed (Sec. III-D). Motions with a walking sequence were identified for speeds as low as 0.12 m/s, while no running sequence for velocities lower than 0.50 m/s with the knees pointing forward and lower than 0.90 m/s with the knees pointing backwards were identified.

At a velocity of 1.04 m/s a clear transition point in terms of the CoT-optimal footfall pattern is observed, changing from a walking sequence to a running sequence. For motions with a running sequence, the rate of increase of the CoT was drastically reduced beyond this transition point. In contrast, the CoT of motions with a walking sequence kept growing at an increasing rate. As detailed in the subsequent sections, this divergence corresponds to a sudden and discrete transition in terms of the underlying gait characteristics.

A. Ballistic Walking at Speeds Below 1.04 m/s

Motions with a walking sequence were energetically the most efficient at speeds below 1.04 m/s. When examining the exchange of kinetic, gravitational, and elastic energy content over the course of a stride, the motions exhibited a clear *out of phase* transfer between kinetic and gravitational energy (Fig. 4). Additionally, gravitational energy was highest during mid-stance with the center of mass moving in an upwards arc. There was virtually no elastic energy storage in motions with the knees pointing forward. Some energy was stored elastically in motions with the knees pointing backwards. The ground reaction forces (Fig. 5) were mostly flat apart from a large peak at the beginning of single stance (an effect of the contact collision). With the knees pointing forward, a peak in force towards the end of stance, reminiscent of a human push-off, was discovered. This is consistent with the demonstrated energetic benefit of pre-emptive push-off for both animals [27] and machines [28].

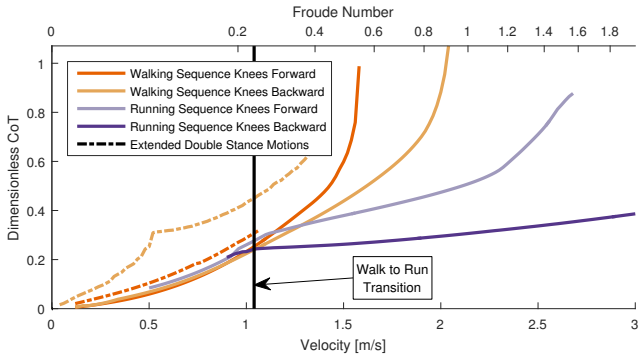

Fig. 2. Cost of transport is shown as a function of speed given in m/s and as a non-dimensional Froude number: $F = \frac{v^2}{g\ell}$ (where $\ell = 0.47\,\mathrm{m}$ is the extended leg length of the robot). At all speeds, the walking sequences with an extended double stance phase were suboptimal compared to those with instantaneous support transfer. As such, the remainder of the analysis focuses on walking sequences with zero double support phase. At low speeds, all four remaining cases had a similar CoT. Walking footfall sequences had a slight energetic advantage. For speeds below 0.88 m/s, the walking sequences with the knees pointing forward had the lowest CoT, for speeds between 0.88 m/s and 1.04 m/s it became optimal for knees to point backwards. Motions with a running footfall sequence were slightly more energetically expensive below 1.04 m/s. However, their CoT was only up to 0.036 higher. At high speeds above 1.04 m/s, the CoT of the four gaits diverged. Moving with a running sequence and with the knees pointing backwards became by far the most efficient mode of locomotion. Using a walking sequence increased the CoT by up to 0.77 (259 %) at 2.04 m/s. Having the knees point forward instead of backward increased the CoT of the running sequence by up to 0.52 (148 %) at 2.68 m/s.

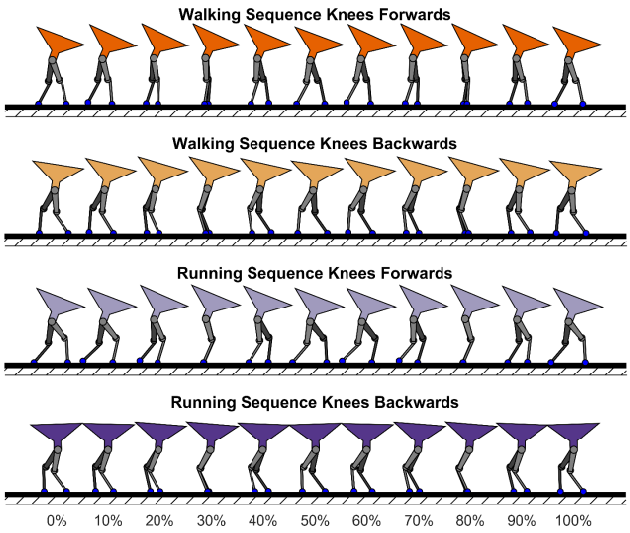

Fig. 3. Video stills show the optimal motions at a speed of 0.9 m/s. This speed is below the walk to run transition and the gaits share similar properties that are indicative of ballistic walking. In particular, the knees are extended, the main body is pitched forward, and the center of mass moves in an upwards arc. The running sequence with knees pointing backwards is an exception to this pattern and shows characteristics more reminiscent of Groucho running.

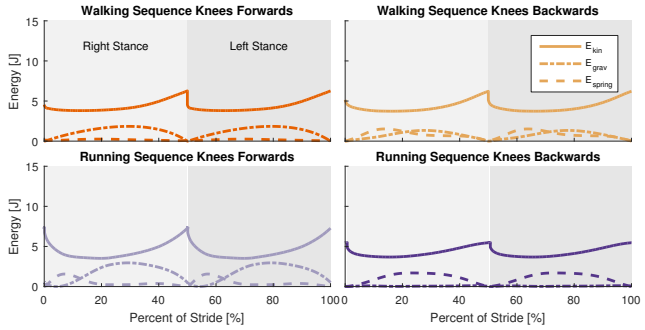

Fig. 4. Center of mass kinetic, gravitational, and elastic energy flow for all motions at 0.9 m/s. Both walking sequence motions and the knees forward running sequence motion exhibit an out-of-phase relationship between kinetic and potential energy. This is prototypical of ballistic walking [29]. The knees backwards running sequence gait exhibits Groucho running [31], characterized by a constant potential energy and an out of phase exchange between kinetic and elastic energy.

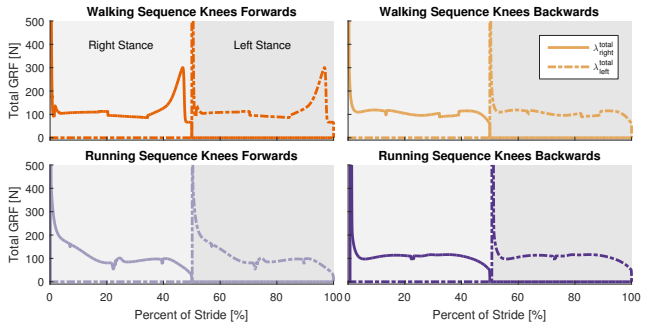

Fig. 5. Ground reaction force magnitudes at 0.9 m/s. A distinct pushoff force is observed near the end of each single stance phase for the knees forward walking sequence. This pushoff force is conspicuously absent in the other three motions.

The characteristics of the energy exchange are clearly indicative of *ballistic walking* [29]. Especially with the knees pointing forward, the robot's optimal motion is much like that of a compass gait walker [30] with almost no energy storage in the elastic actuators and the dynamics represent those of an inverted pendulum. This is in stark contrast to earlier studies with simplified models of robotic systems, which found that at low speeds, elastic walking with substantial elastic energy storage in leg springs and an extended double support was the optimal locomotion mode [16]. The absence of elastic walking gaits [11], [16] in RAM*one*'s motion is likely a consequence of the fact that the knees are nearly straight throughout stance (Fig. 3 and supplementing video) which makes the robot's legs rigid. This knee extension is not as pronounced when the knees are pointing backwards and more storage of elastic energy was observed in this configuration. While the two walking sequences shared many conceptual properties, there remained some visible differences including varying amounts of elastic energy storage throughout the gait, straightness of the knees, stride length, and stride frequency. However, overall both motions were clearly ballistic walking gaits.

For motions with a running sequence, the outcome was more structurally dependent on the knee direction. With the knees pointing backwards, the duration of the air-phase was nearly zero and the energy dynamics showed an exchange between kinetic and elastic energy storage, with hardly any fluctuations in gravitational energy (Fig. 4). This gait could be described as *Groucho running* [31]. However, only such motions for speeds larger than 0.90 m/s could be found. In contrast, with the knees pointing forwards, such motions were found for speeds as low as 0.50 m/s. These motions showed all characteristics of ballistic walking, even though they had a running footfall sequence. Characteristics included an out-of-phase relationship in kinetic and gravitational energy (Fig. 4), an upwards arc of the center of mass, and extended knees (Fig. 3). The optimizer brought the air-phase duration of these gaits nearly to zero (Fig. 6), getting as close as possible to an instantaneous transfer of support.

One should note that there is an important difference between a walking sequence with a zero duration double support and a running sequence with a zero duration air-phase. In the walking sequence, the touchdown impact at the leading leg and the resulting impulse that propagates through the mechanical structure create an immediate lift-off of the trailing leg. When we enforce an air-phase (even of vanishing time duration), the trailing leg must leave the ground before the impact collision, meaning that lift-off must be generated without the assistance of the ground impulse. Despite this important difference, the optimizer still converged to a ballistic walking motion.

B. Spring-Mass Running at Speeds Above 1.04 m/s

As locomotion speed was increased beyond 1.04 m/s, a sudden and significant increase in the air-phase duration was observed for motions with a running footfall sequence (Fig. 6). With knees pointing backwards, for example, the air-phase duration (as percentage of a full stride) increased in a single velocity increment from 1.3 % at 1.04 m/s to 18.6 % at 1.06 m/s. The sudden increase is indicative of a structural change in the motion strategy. For speeds larger than 1.04 m/s, the energy flows of these motions exhibited an *in phase* relationship between kinetic and gravitational energy, with energy being stored as elastic energy in the actuator springs (Fig. 8). Gravitational energy was lowest at mid-stance with the center of mass moving in a downwards arc. For both knee orientations, the ground reaction forces showed an initial (collision) peak followed by a single hump (Fig. 9).

These characteristics are clearly indicative of *spring-mass running*, also called *spring loaded inverted pendulum (SLIP) running* [10]. The legs are used as springs and the motion resembles that of a bouncing ball. The required leg-compliance is achieved by a more pronounced knee bend that softens the leg (Fig. 7 and supplementing video).

In contrast to the sudden changes that were observed in motions with a running sequence, motions with a walking sequence remained mostly unchanged across the transition point. In particular, they continued to exhibit an instantaneous transfer of support, extended knees, and all other characteristics of a ballistic walking gait.

C. Walk to Run Transition

At the transition point, the most economical footfall sequence changed from a walking sequence to a running se-

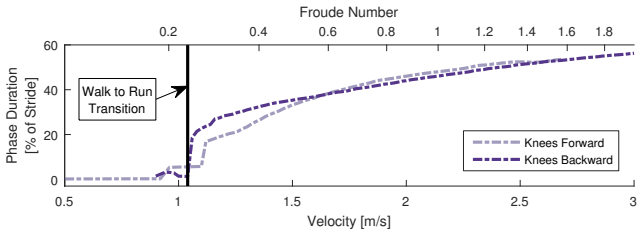

Fig. 6. Flight phase durations of the running sequences. The optimal flight phase duration is near zero for speeds below the walk to run transition and jumps up sharply at speeds above this point, indicating a sudden and discrete change in gait.

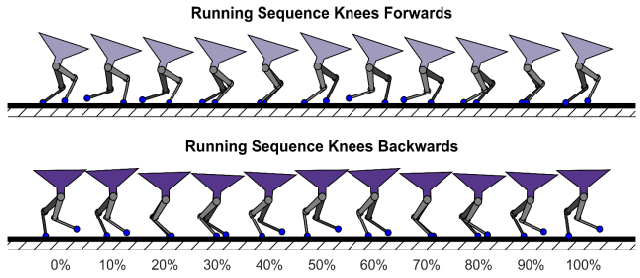

Fig. 7. Video stills of the optimal running sequence motions at 1.2 m/s. In contrast to the same footfall sequence at lower speeds (Fig. 3), the motions now exhibit clear properties of spring-mass running. This includes a pronounced knee bend and a downwards arc of the center of mass.

quence. This change in footfall sequence was not the only indication of gait change. When considering only motions with a running sequence, we observed a clear structural change at this speed. Below this speed, the motion with forward knees closely resembled a ballistic walking gait, despite the presence of an enforced air-phase. The energetic benefits of changing gait thus likely do not originate primarily in the footfall sequence, but more in the dynamic pattern of the

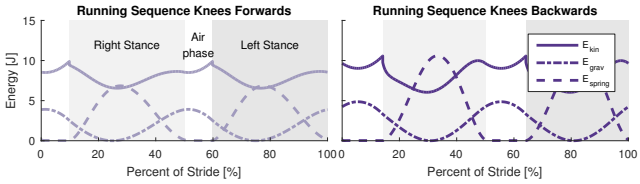

Fig. 8. Center of mass kinetic, gravitational, and elastic energy flow for running sequence motions at 1.2 m/s. The left and right contact phases of the motion are indicated with a shaded background. Both motions exhibit the in-phase kinetic and gravitational energy oscillation with out of phase elastic energy that characterizes spring mass running [10].

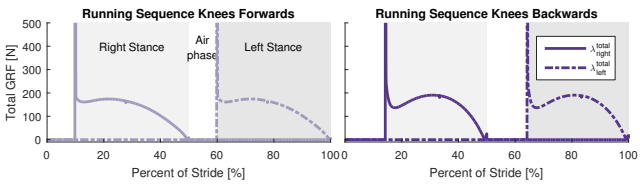

Fig. 9. Total ground reaction force at each foot for running sequence motions at 1.2 m/s. Both knees forward and backwards motions exhibit a sharp initial force at contact followed by a single hump.

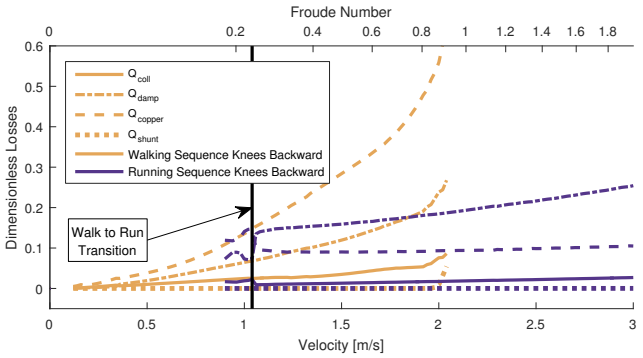

Fig. 10. Comparison of loss contributions (normalized by $mg\Delta x$) between walking and running sequences . Results are shown across a range of speeds and for motions with the knees pointing backwards. All components of the walking sequence motion increase smoothly across speed, with electrical losses dominating. In contrast, the individual costs of the running sequence motion change discretely across the walk to run transition. Below the transition, the costs of the running sequence motion roughly follow those of the walking sequence motion. Above the transition, the electrical losses sharply decrease and damping losses dominate the cost. This sharp jump is a result of the transition from *Groucho running* to spring mass running.

chosen gait.

The transition occurred at a Froude number of 0.23. This is similar to the 0.25 observed for a simple biped in [16], but is significantly smaller than the 0.42 observed for humans [8]. Additionally, the transition speed is similar for both forwards and backwards knee directions. The similarity of the transition speed between the two knee orientations and the prismatic legs of [16] suggests the existence of an underlying trigger that is independent of leg morphology.

What is this mechanism that drives the sudden structural change in motion at speeds of 1.04 m/s? Why is ballistic walking more efficient at lower speeds and why is spring-mass running more efficient at higher speeds? One hypothesis is proposed in [8], where the authors found a similar transition for a minimal biped model. They argued that this was driven by the large collision cost of high speed ballistic walking.

In order to see if similar arguments apply to our results, we separated the total CoT into losses due to collisions, damping losses, copper losses, and shunt losses. Since the motion trajectories were periodic, no energy was gained or lost by the robot over one period, and the energy required to drive the actuators matched the above mentioned losses:

$$c = Q_{coll} + Q_{damp} + Q_{copper} + Q_{shunt}. \tag{7}$$

To match the definition of the CoT, the values of these losses were scaled by $(mg\Delta x)^{-1}$.

This breakdown of contributors to overall cost was computed for motions with the knees pointing backwards in both a walking and a running sequence (Fig. 10). For the walking sequence, copper losses were the primary contributor to the cost (on average 57 %), followed by damping losses (31 %) and collision losses (13 %). A similar breakdown was obtained for the running sequence below 1.04 m/s. For the running sequence above 1.04 m/s, this ratio was inverted, damping losses led (on average 62 %), followed by copper losses (31 %) and collision losses (6 %). Negative electrical work appeared solely in high speed walking sequence gaits.

The fact that collision losses were dominated by damping and electrical losses in our cost function would indicate that the mechanism proposed in [8] is not the sole factor driving the walk to run transition.

D. Influence of the Knee Direction

A notable finding was the large difference in CoT as a function of knee direction. For the running sequence, moving with forwards knees required on average 60 % more energy than with backwards knees. This is in agreement with prior findings in [32], in which it was shown that backwards kneed gaits are more efficient for most five link bipeds.

The increased cost for forward kneed running is incurred during leg retraction at the beginning of swing. Since the reflected rotor inertia for this robot is large in comparison to the leg mass, the majority of the cost of leg retraction comes from reversing the direction of the motors.

For the knee backwards gait, the push-off velocity is largely generated from the extension of the knee joint (kinematically governed by the liftoff speed). This velocity can be driven by the knee springs, allowing the motors to begin moving in flexion even before liftoff (Fig. 11). As a result, the knee rotors don't need to reverse direction during swing.

For the knee forwards gait, the push-off velocity is mainly generated from the extension of the hip. Ideally this velocity would come from spring deflection (as in the knee), however, this deflection would create a large hip torque before liftoff. Since torques in the hip before liftoff lead to pitching of the main body, the hip spring deflection must be small. This forces the hip motor to match the hip joint velocity (Fig. 11).

Therefore, knee forwards running gaits must quickly dissipate a large angular momentum stored in the hip motors at liftoff in order to retract the swing leg. In this case 1.13 J (0.0157 when expressed as a dimensionless energy) of hip rotor energy must be dissipated. When the knees are pointing backwards, only 0.02 J (0.0004) of energy is dissipated.

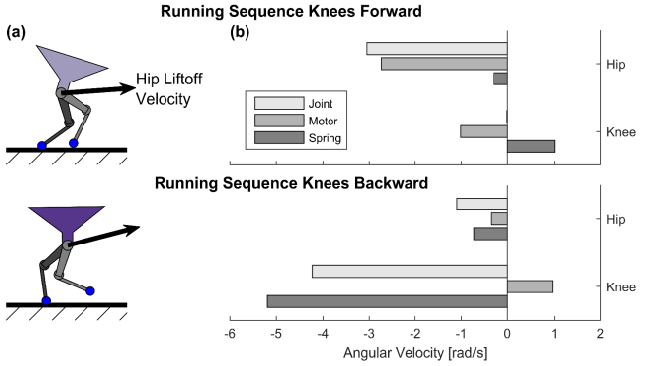

Fig. 11. The different knee directions in the running sequence motion lead to different robot configurations at liftoff (shown in (a) for a velocity of 1.2 m/s). As a consequence, the joint velocities in the swing leg (shown in (b)) differ greatly between the two cases. These joint velocities are the sum of the motor and spring velocities. A significant deflection in the knee springs decouples the joint from the motor. Joint and motor velocities are thus distinctly different, and the knee motor is already moving to retract the leg while the knee joint extends for liftoff. The same does not hold for the hip joint, where joint and motor motion must be more similar and the motor motion can only be reversed after lift-off. Because of this, running with the knees backwards is at an advantage, since it requires a much smaller hip velocity. [Note that all velocities are defined to be positive when counter clockwise. A positive knee velocity thus indicates knee extension when the knees are forward, and knee flexion when the knees are backwards.]

IV. Discussion & Conclusion

This paper presents a study on the question of economical gait selection for legged robotic systems. Optimal control was used to generate energy optimal motions for a realistic model of the bipedal robot RAM*one*. Two different footfall sequences (a walking sequence with a double-support phase and a running sequence with an air-phase) and two different orientations of the knee joints (pointing forwards and backwards) were compared. Actuator inputs and motion trajectories that minimized the electrical cost of transport were identified for a range of velocities. The optimal motion at each individual speed was computed and each such motion was characterized using established gait classifications.

At a speed of 1.04 m/s the optimal gait was found to change from ballistic walking with an instantaneous double-support to spring-mass running with an extended air-phase. Switching from ballistic walking to spring-mass running reduced energy consumption by up to 88 %. *This result illustrates clearly that it is beneficial for RAMone to employ different gaits at different speeds.*

Notably the different motions at distinct speeds distinguished themselves primarily in terms of the dynamics of the motion. Gaits were clearly identified as either ballistic walking or spring-mass running. That is, at low speeds nearly no energy was stored in the actuator springs, while at high speeds almost all of the energy fluctuations within the robot were conducted through the springs. There was no continuous transition between these types, with a sudden change occurring at a speed of 1.04 m/s. This switch was not only initiated by a change of footfall sequence, as motions with a running footfall sequence showed clearly different dynamic behaviors below and above this speed.

That the identified optimal motions shared many properties with gaits found in humans and animals was not expected per-se. While the overall morphology of RAM*one* roughly resembles that of a human (when the knees point forward) or of birds (when the knees point backwards), there are considerable differences between this robot and biological systems. Among these, RAM*one* lacks ankles and feet, is actuated by electrical DC motors which have a considerable reflected inertia, has springs that are only slightly damped, and employs a cost function that trades-off work and force penalties specific to electric actuators. Still, the general trend of transitioning from ballistic walking to spring-mass running, as well as the main characteristics of the individual gaits (especially with respect to the exchange of potential, gravitational, and elastic energy) were similar. Most major differences, such as the lack of the double stance phase found in human walking, were likely a consequence of the rigidity of the robot's structure (which differs from the compliant legs of humans and animals).

It is tempting to interpret the backwards-knee orientation as a transformation of the knees into ankles, thereby making the morphology of the robot more similar to that of, for example,

birds or ungulates. However, this interpretation is not made in this paper since, unlike animals, the inertia of RAM*one*'s leg is largely dominated by the reflected inertia of the actuators (by a factor of 10). Still, the demonstrated benefits left no doubt that RAM*one* should locomote with knees pointing backwards.

It is necessary to note that the optimization problems in this paper are not convex. Relying on local methods, we cannot guarantee that our results represent globally optimal motions. However, despite seeding each contact sequence and knee orientation with dissimilar initial trajectories, all four optimizations converged to similar gaits with similar cost of transport at low speeds. For the running sequence, this means that optimizations seeded with locally optimal ballistic running gaits converged instead to pendular walking gaits at speeds below the walk to run transition. Since walking and running have discretely different trajectories, there is likely no sequence of locally optimal gaits that lead gradually from the first local minimum to the other. This indicates that our search is capable of escaping suboptimal local minima.

This work prompts several questions that merit further investigation. One is that of generality. How do these results extend to other robots? Another is gait transition. What drives the transition in RAM*one*, and why does it occur at similar speeds across leg morphologies? We also hope to understand specific features of the gaits, such as the significantly bent knee at liftoff and touchdown during knees forward running.

Additionally, while we did our best to model RAM*one* as precisely as possible, certain effects can never fully be encoded in a simulation. This includes gearbox friction, foot deformation, elastic forces in cables, and parametric model error. To truly appreciate the role and benefits of using different gaits in legged robots, one thus has to implement optimal gaits on an actual robotic prototype.

This study is another milestone in the effort to understand the meaning and the usefulness of different gaits in legged robotic systems. It extends on an understanding of biology [1], [4], simple passive models [11], [12] and conceptual models [16], and adds a strong layer of realism to this question. It now remains to explore how these results translate to actual physical robots.

REFERENCES

[1] D. F. Hoyt and C. R. Taylor, "Gait and the energetics of locomotion in horses," *Nature*, vol. 292, no. 5820, pp. 239–240, 1981.

[2] R. Margaria, *Sulla fisiologia e specialmente sul consumo energetico della marcia e della corsa a varie velocita ed inclinazioni del terreno*. 1938.

[3] M. Hildebrand, "The adaptive significance of tetrapod gait selection," *Integrative and Comparative Biology*, vol. 20, no. 1, pp. 255–267, 1980.

[4] G. A. Cavagna, N. C. Heglund, and C. R. Taylor, "Mechanical work in terrestrial locomotion: two basic mechanisms for minimizing energy expenditure," *American Journal of Physiology-Regulatory, Integrative and Comparative Physiology*, vol. 233, no. 5, pp. R243–R261, 1977.

[5] R. M. Alexander, "A model of bipedal locomotion on compliant legs," *Philosophical Transactions of the Royal Society of London B: Biological Sciences*, vol. 338, no. 1284, pp. 189–198, 1992.

[6] M. Hutter, C. D. Remy, M. A. Hoepflinger, and R. Siegwart, "High compliant series elastic actuation for the robotic leg scarleth," in *International Conference on CLimbing And WAlking Robots, CLAWAR*, 2011.

[7] K. Green, N. Smit-Anseeuw, R. Gleason, and C. D. Remy, "Design and control of a recovery system for legged robots," in *2016 IEEE/ASME international conference on Advanced intelligent Mechatronics*, pp. 1–6, IEEE, 2016.

[8] M. Srinivasan and A. Ruina, "Computer optimization of a minimal biped model discovers walking and running," *Nature*, vol. 439, no. 7072, pp. 72–75, 2006.

[9] T. McGeer, "Passive dynamic walking," *The International Journal of Robotics Research*, vol. 9, no. 2, pp. 62–82, 1990.

[10] R. Blickhan, "The spring-mass model for running and hopping," *Journal of biomechanics*, vol. 22, no. 11-12, pp. 1217–1227, 1989.

[11] H. Geyer, A. Seyfarth, and R. Blickhan, "Compliant leg behaviour explains basic dynamics of walking and running," *Proceedings of the Royal Society of London B: Biological Sciences*, vol. 273, no. 1603, pp. 2861–2867, 2006.

[12] Z. Gan, T. Wiestner, M. A. Weishaupt, N. M. Waldern, and C. D. Remy, "Passive dynamics explain quadrupedal walking, trotting, and tölting," *Journal of Computational and Nonlinear Dynamics*, vol. 11, no. 2, p. 021008, 2016.

[13] C. D. Remy, *Optimal Exploitation of Natural Dynamics in Legged Locomotion*. PhD thesis, Eidgenssische Technische Hochschule, 2011.

[14] M. Srinivasan, "Fifteen observations on the structure of energy-minimizing gaits in many simple biped models," *Journal of The Royal Society Interface*, p. rsif20090544, 2010.

[15] W. Xi and C. D. Remy, "Optimal gaits and motions for legged robots," in *Intelligent Robots and Systems (IROS 2014), 2014 IEEE/RSJ International Conference on*, pp. 3259–3265, IEEE, 2014.

[16] W. Xi, Y. Yesilevskiy, and C. D. Remy, "Selecting gaits for economical locomotion of legged robots," *The International Journal of Robotics Research*, p. 0278364915612572, 2015.

[17] P. Channon, S. Hopkins, and D. Pham, "Derivation of optimal walking motions for a bipedal walking robot," *Robotica*, vol. 10, no. 02, pp. 165–172, 1992.

[18] C. Chevallereau and Y. Aoustin, "Optimal reference trajectories for walking and running of a biped robot," *Robotica*, vol. 19, no. 05, pp. 557–569, 2001.

[19] T. Yang, E. Westervelt, J. P. Schmiedeler, and R. Bockbrader, "Design and control of a planar bipedal robot ernie with parallel knee compliance," *Autonomous robots*, vol. 25, no. 4, pp. 317–330, 2008.

[20] M. Hutter, C. D. Remy, M. A. Hoepflinger, and R. Siegwart, "Scarleth: Design and control of a planar running robot," in *Intelligent Robots and Systems (IROS), 2011 IEEE/RSJ International Conference on*, pp. 562–567, IEEE, 2011.

[21] C. D. Remy, M. Hutter, M. Hoepflinger, M. Bloesch, C. Gehring, and R. Siegwart, "Quadrupedal robots with stiff and compliant actuation," *at-Automatisierungstechnik Methoden und Anwendungen der Steuerungs-, Regelungs-und Informationstechnik*, vol. 60, no. 11, pp. 682–691, 2012.

[22] R. Goebel, R. Sanfelice, and A. Teel, "Hybrid dynamical systems," *Control Systems Magazine, IEEE*, vol. 29, no. 2, pp. 28–93, 2009.

[23] G. Gabrielli and T. Von Karman, *What price speed?: specific power required for propulsion of vehicles*. 1950.

[24] H. G. Bock and K.-J. Plitt, "A multiple shooting algorithm for direct solution of optimal control problems," PROCEEDINGS OF THE IFAC WORLD CONGRESS, 1984.

[25] D. Leineweber, "Efficient reduced sqp methods for the optimization of chemical processes described by large sparse dae models," 1999.

[26] M. Diehl, D. B. Leineweber, and A. A. Schäfer, *MUSCOD-II User's Manual*. IWR, 2001.

[27] S. J. Hasaneini, C. J. Macnab, J. E. Bertram, and H. Leung, "Optimal relative timing of stance push-off and swing leg retraction," in *2013 IEEE/RSJ International Conference on Intelligent Robots and Systems*, pp. 3616–3623, IEEE, 2013.

[28] A. Ruina, J. E. Bertram, and M. Srinivasan, "A collisional model of the energetic cost of support work qualitatively explains leg sequencing in walking and galloping, pseudo-elastic leg behavior in running and the walk-to-run transition," *Journal of theoretical biology*, vol. 237, no. 2, pp. 170–192, 2005.

[29] S. Mochon and T. A. McMahon, "Ballistic walking: An improved model," *Mathematical Biosciences*, vol. 52, no. 3, pp. 241–260, 1980.

[30] V. T. Inman, H. D. Eberhart, *et al.*, "The major determinants in normal and pathological gait," *J Bone Joint Surg Am*, vol. 35, no. 3, pp. 543–558, 1953.

[31] T. A. McMahon, G. Valiant, and E. C. Frederick, "Groucho running," *Journal of Applied Physiology*, vol. 62, no. 6, pp. 2326–2337, 1987.

[32] M. Haberland and S. Kim, "On extracting design principles from biology: Ii. case studythe effect of knee direction on bipedal robot running efficiency," *Bioinspiration & biomimetics*, vol. 10, no. 1, p. 016011, 2015.